

## Comparative Numerical Analysis of the Tungsten Transport in Drift Optimized Stellarator Ergodic and Nonergodic Plasma Configurations

Oleg A. SHYSHKIN<sup>1</sup>, Ralf SCHNEIDER<sup>2</sup>, Craig BEIDLER<sup>2</sup>

<sup>1</sup>Kharkov "V.N.Karazin" National University, Svobody sqr.4, Kharkov-77, 61077, UKRAINE

<sup>2</sup>Max-Planck-Institut für Plasmaphysik, EURATOM Assosiation, Teilinstitut Greifswald, D-1791 Greifswald, GERMANY

The radial transport of tungsten ions is studied for two magnetic field configurations, ergodic and nonergodic, in the HELIAS stellarator with five periods of the magnetic field under finite plasma pressure parameter  $\beta = 3\%$ . The ergodic magnetic field configuration is represented with the use of additional magnetic field perturbations, which create the stochastic layer at the radial position  $2/3$  of plasma radius. Coulomb scattering of the tungsten ions on the background plasma particles (electrons, deuterons and tritons) is simulated by means of discretized collisional operator.

### MAGNETIC FIELD MODEL AND GUIDING CENTER EQUATIONS

For the numerical treatment we use the magnetic coordinates  $(\psi, \vartheta, \zeta)$  [1]. In case of closed nested magnetic surfaces the magnetic field strength can be represented in the series

$$B = 1 + \sum_{k=0}^{\infty} b_{0,k}(r_p) \cos(Mk\zeta) + \sum_{l=1}^{\infty} \sum_{k=-\infty}^{\infty} b_{l,k}(r_p) \cos(Mk\zeta - l\vartheta), \quad (1)$$

where Fourier coefficients  $b_{l,k}(r_p) = \sum_{n=0}^3 b_{l,k,n} r_p^n$  are the functions of the normalized small radius  $r_p$  of the torus and  $M$  is the number of the magnetic field periods along the torus. To

represent the magnetic field strength in HELIAS stellarator configuration under plasma pressure  $\beta = 3\%$  we use the set of eight Fourier coefficients [2]. The exact magnetic field  $B_e$  that possesses the isolated islands and stochastic layers can be presented as  $B_e = B + \nabla \times \alpha B$  with  $B$  having exact, nested, magnetic surfaces [3]. The perturbation function of the form [4]

$$\alpha = \sum_{n,m} A_{n,m} \left( r/a_{m,n} \right)^m \left( a_{pl} - r \right)^p / \left( a_{pl} - a_{m,n} \right)^p \sin(n\zeta - m\vartheta - \omega_{n,m} \tau + \delta_{n,m}) \quad (2)$$

gives us possibility to vary the amplitude of perturbation  $A_{n,m}$ , "wave" numbers  $m$  and  $n$ , perturbation frequency  $\omega_{n,m}$  and to create different magnetic field structures. The amplitude peak of the perturbation takes place at  $a_{m,n}/a_{pl} = m/(m+p)$ , where  $a_{m,n}$  is the radius of the rational magnetic surface with rotational transform  $t = n/m$  and  $a_{pl}$  is the plasma radius.

The integration of the guiding center equations [4],

$$\dot{\psi} = \rho_{\parallel} \frac{\partial \alpha}{\partial \vartheta} B^2 - (\rho_{\parallel}^2 B + \mu) \frac{\partial B}{\partial \vartheta}, \quad (3)$$

$$\dot{g} = \rho_{\parallel} B^2 \left( \iota - \frac{\partial \alpha}{\partial \psi} \right) + \frac{\partial \Phi}{\partial \psi} + (\mu + \rho_{\parallel}^2 B) \frac{\partial B}{\partial \psi}, \quad (4)$$

$$\dot{\zeta} = \rho_{\parallel} B^2, \quad (5)$$

$$\dot{\rho}_{\parallel} = (\rho_{\parallel}^2 B + \mu) \left[ \left( -\iota + \frac{\partial \alpha}{\partial \psi} \right) \frac{\partial B}{\partial \vartheta} - \frac{\partial \alpha}{\partial \vartheta} \frac{\partial B}{\partial \psi} - \frac{\partial B}{\partial \zeta} \right] - \frac{\partial \Phi}{\partial \psi} \frac{\partial \alpha}{\partial \vartheta}, \quad (6)$$

is performed by mean of Runge-Kutta method. These equations include the magnetic field perturbation function  $\alpha$  and only the radial electric field that is presented by term  $\partial \Phi / \partial \psi \neq 0$ .

### DISCRETIZED COLLISION OPERATOR

To present a collisional kick in energy and pitch angle ( $\lambda = v_{\parallel} / v$ ), which particle gets after each integration time step, the discretized collision operator is used [5]. The operator for tungsten ions, colliding with the background plasma particles, electrons, deuterons and tritons has the form for the pitch angle scattering

$$\lambda_n = \lambda_0 (1 - \nu_d \delta \tau) \pm \sqrt{(1 - \lambda_0^2) \nu_d \delta \tau}, \quad (7)$$

where  $\nu_d = \sum_{k=e,D,T} \nu_d^{W/k}$ , and for the energy slowing down and scattering

$$K_n = K_0 - 2 \delta t \sum_{k=e,D,T} \nu_K^{W/k} \left[ K_0 - X^{W/k} \Psi'(X^{W/k}) T_k / \Psi(X^{W/k}) \right] \pm 2 \sqrt{K_0 \delta t \sum_{k=e,D,T} \nu_K^{W/k} T_k}. \quad (8)$$

The subscripts “n” and “o” mean new and old respectively, and  $\delta \tau$  is integration time step.

Collision frequencies  $\nu_d^{W/k}$ ,  $\nu_K^{W/k}$  are represented through the Maxwell integral  $\Psi(X^{W/k})$ ,

where  $X^{W/k} \equiv (v_w / \sqrt{2T_k / m_k})^2$ .

### CORONAL MODEL

In a general time-dependent situation the number density of the charge state  $Z$  for the impurity ion satisfies the following equation

$$\frac{dN(Z)}{dt} = n_e \left[ -S(Z)N(Z) - \alpha(Z)N(Z) + S(Z-1)N(Z-1) + \alpha(Z+1)N(Z+1) \right] \quad (9)$$

Here  $n_e$  is background electrons density and  $S(Z)$  is the ionization rate. The recombination rate  $\alpha(Z)$  has the form  $\alpha(Z) = \alpha_r + \alpha_d$ , where  $\alpha_r$  and  $\alpha_d$  are the radiative and dielectronic recombination rates respectively. Under steady state condition  $dN(Z)/dt = 0$  the equation (9)

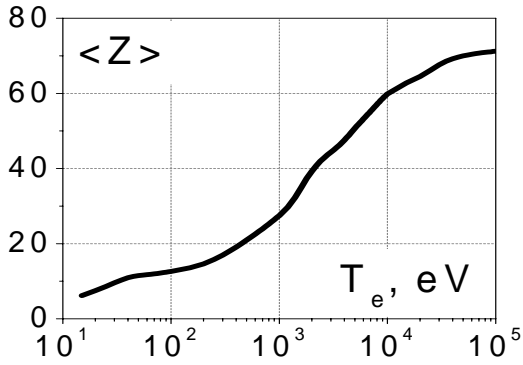


Fig. 1. Average charge state of the tungsten ion ensemble versus electron temperature.

presents the corona model [6] that can be used to calculate the average charge state of tungsten ion ensemble in the form

$$\langle Z \rangle = \frac{\sum_i N(i)i}{\sum_i N(i)}. \quad (10)$$

On figure 1 the average charge state of the tungsten ion versus background electron temperature is presented for an average electron density  $n_e = 5 \times 10^{13} \text{ cm}^{-3}$ .

### TUNGSTEN TRANSPORT IN HELIAS PLASMA CONFIGURATIONS

The temperature and density profiles in HELIAS reactor nonergodic configuration  $\beta = 3\%$ , which are modeled by a simple analytic formula, are shown on figure 2. On figure 3

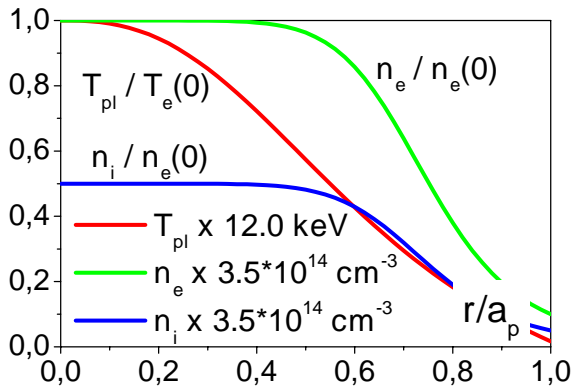


Fig. 2. Plasma profiles in HELIAS stellarator nonergodic configuration.

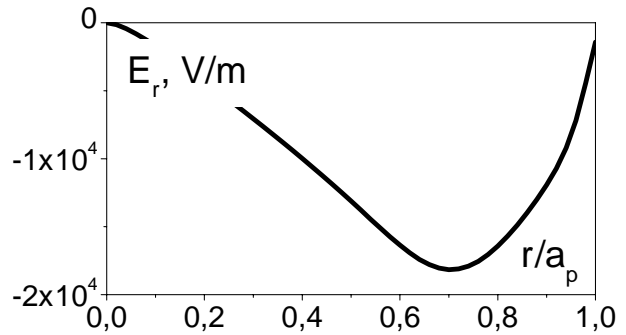


Fig. 3. Radial electric field profile in HELIAS stellarator nonergodic configuration.

the radial electric field profile, which is evaluated by mean of equating the particle fluxes, is shown.

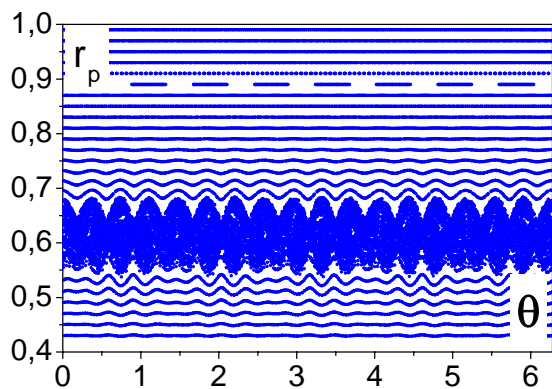


Fig. 4. Magnetic surfaces with a stochastic layer in HELIAS stellarator.

The ergodic magnetic field configuration is created with the use of additional magnetic field perturbations  $m_1/n_1 = 17/14$  and  $m_2/n_2 = 22/18$  to create the island chains, which overlap and give raise to the stochastic layer at the radial position  $2/3$  of plasma radius (figure 4).

Plasma profiles, which correspond to the stochastic magnetic field configuration, are shown on figure 5. Background electron and ion density profiles stay unchanged and the temperature profile has flattening in the area of the ergodic region. On figure 6 the radial electric field profile calculated for a stochastic configuration is presented. 10000 tungsten ions

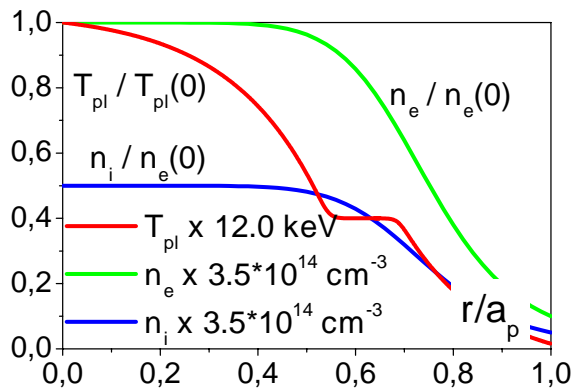


Fig. 5. Plasma profiles in HELIAS stellarator ergodic configuration.

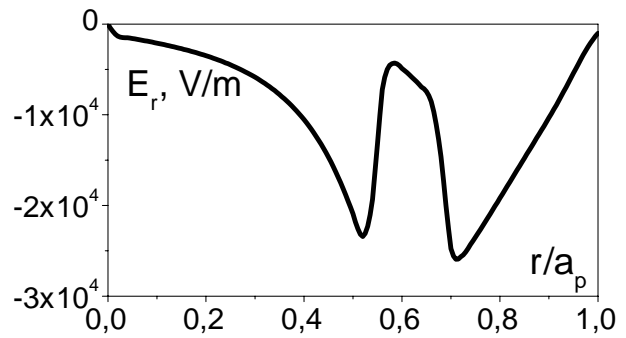


Fig. 6. Radial electric field profile in HELIAS stellarator ergodic configuration.

with start parameters  $r_0/a_p = 0.8$ ,  $\lambda_0 = 0.5$  and energy is equal to the plasma temperature

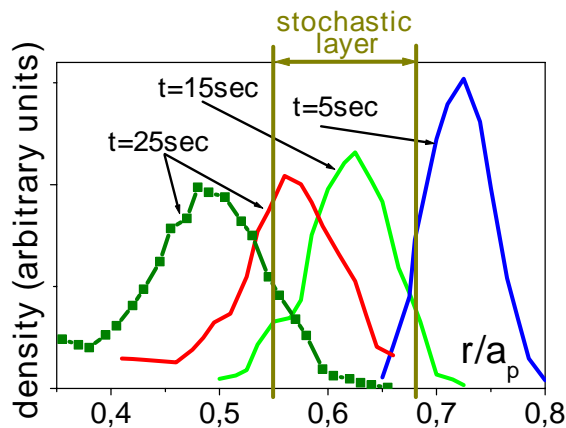


Fig. 7. Tungsten ion profiles in HELIAS stellarator, ergodic (blue, green, red) and nonergodic (olive) configurations.

were traced during 25 seconds. On figure 7 the evolution of impurity profile is presented for ergodic (lines) in different time slices and nonergodic (line with symbols) configurations. It is shown that in nonergodic case impurities drift towards the plasma core faster than in presence of ergodic layer. One can conclude that stochastic layer acts as an impediment to tungsten accumulation.

### CONCLUSIONS

A new transport code is developed. This code gives possibility to trace impurity particles in different plasma configurations, which include stochastic layers of the magnetic field. Comparison analyses of tungsten ions transport leads to conclusion that stochastic layer decreases diffusion of impurity ions with a high charge state towards a plasma core and can be used as an impediment to tungsten accumulation.

<sup>1</sup>W.D. D'haeseller, W.N.G. Hitchon, J.D. Callen, et al, Flux Coordinates and Magnetic Field Structure // Springer-Verlag Berlin Heidelberg, 1991.

<sup>2</sup>C.D. Beidler, (1996) Proceedings of the 6<sup>th</sup> Workshop on WENDELSTEIN 7-X and Helias Reactor, January, IPP 2/331. -P. 194.

<sup>3</sup>A.H. Boozer, R.B. White, (1982) Princeton Plasma Physics Laboratory Report PPPL-1872, -pp. 1-16.

<sup>4</sup>A.A. Shishkin, I.N. Sidorenko, H. Wobig, (1998) J. Plasma Fusion Res. SERIES, **1**, 480

<sup>5</sup>William D. D'haeseleer and Craig D. Beidler, (1993) Computer Phys. Communications **76**, 1

<sup>6</sup>K. Asmussen, K.B. Fournier, J.M. Laming, et al, (1998) Nuclear Fusion, **38**, 967